The Astrophysical Journal, 805:187 (8pp), 2015 June 1 doi:10.1088/0004-637X/805/2/187

A MISSING-LINK IN THE SUPERNOVA–GRB CONNECTION: THE CASE OF SN 2012ap

Sayan Chakraborti[1,2], Alicia Soderberg[1], Laura Chomiuk[3], Atish Kamble[1], Naveen Yadav[4], Alak Ray[4], Kevin Hurley[5], Raffaella Margutti[1], Dan Milisavljevic[1], Michael Bietenholz[6,7], Andreas Brunthaler[8], Giuliano Pignata[9], Elena Pian[10], Paolo Mazzali[11,12], Claes Fransson[13], Norbert Bartel[7], Mario Hamuy[14], Emily Levesque[15], Andrew MacFadyen[16], Jason Dittmann[1], Miriam Krauss[17], M. S. Briggs[18], V. Connaughton[18], K. Yamaoka[19], T. Takahashi[20], M. Ohno[21], Y. Fukazawa[21], M. Tashiro[22], Y. Terada[22], T. Murakami[23], J. Goldsten[24], S. Barthelmy[25], N. Gehrels[25], J. Cummings[25,26], H. Krimm[25,27], D. Palmer[28], S. Golenetskii[29], R. Aptekar[29], D. Frederiks[29], D. Svinkin[29], T. Cline[30], I. G. Mitrofanov[31], D. Golovin[31], M. L. Litvak[31], A. B. Sanin[31], W. Boynton[32], C. Fellows[32], K. Harshman[32], H. Enos[32], A. von Kienlin[33], A. Rau[33], X. Zhang[33], and V. Savchenko[34]
[1] Institute for Theory and Computation, Harvard-Smithsonian Center for Astrophysics, 60 Garden Street, Cambridge, MA 02138, USA; schakraborti@fas.harvard.edu
[2] Society of Fellows, Harvard University, 78 Mt. Auburn Street, Cambridge, MA 02138, USA
[3] Department of Physics and Astronomy, Michigan State University, East Lansing, MI 48824, USA
[4] Tata Institute of Fundamental Research, 1 Homi Bhabha Road, Mumbai 400005, India
[5] Space Sciences Laboratory, University of California, 7 Gauss Way, Berkeley, CA 94720, USA
[6] Department of Physics and Astronomy, York University, 4700 Keele St., M3J 1P3 Ontario, Canada
[7] Hartebeesthoek Radio Astronomy Observatory, PO Box 443, Krugersdrop, 1740, South Africa
[8] Max-Planck-Institut für Radioastronomie, Auf dem Hügel 69, D-53121 Bonn, Germany
[9] Departamento de Ciencias Fisicas, Universidad Andres Bello, Avda. Republica 252, Santiago, Chile
[10] Scuola Normale Superiore, Piazza Dei Cavalieri 7—I-56126 Pisa, Italy
[11] Liverpool John Moores University, IC2, 146 Brownlow Hill, Liverpool, UK
[12] Max-Planck Institute for Astrophysics, Karl-Schwarzschild-Str. 1, D-85748 Garching, Germany
[13] Department of Astronomy, Stockholm University, AlbaNova, SE-106 91 Stockholm, Sweden
[14] Departamento de Astronoma, Universidad de Chile, Chile
[15] University of Colorado, C327A, Boulder, CO 80309, USA
[16] New York University, 4 Washington Place, New York, NY 10003, USA
[17] National Radio Astronomy Observatory, P.O. Box 0, Socorro, NM 87801, USA
[18] The Center for Space Plasma and Aeronomic Research, University of Alabama in Huntsville, Huntsville, AL 35899, USA
[19] Graduate School of Science, Nagoya University, Furo-cho, Nagoya 464-8602, Japan
[20] ISAS JAXA, 3-1-1 Yoshinodai, Chuo-ku, Sagamihara, Kanagawa 252-5210, Japan
[21] Hiroshima University, 1-3-1 Kagamiyama, Higashi-Hiroshima, Hiroshima 739-8526, Japan
[22] Saitama University, 255 Shimo-Okubo, Sakura-ku, Saitama-shi, Saitama 338-8570, Japan
[23] Kanazawa University, Kadoma-cho. Kanazawa, Ishikawa 920-1192, Japan
[24] Applied Physics Laboratory, Johns Hopkins University, Laurel, MD 20723, USA
[25] NASA Goddard Space Flight Center, Greenbelt, MD 20771, USA
[26] UMBC Physics Department, 1000 Hilltop Circle, Baltimore, MD 21250, USA
[27] Universities Space Research Association, 10211 Wincopin Circle, Columbia, MD 20144, USA
[28] Los Alamos National Laboratory, Los Alamos, NM 87545, USA
[29] Ioffe Physical Technical Institute, St. Petersburg, 194021, Russia
[30] Emeritus, NASA Goddard Space Flight Center, Greenbelt MD 20771, USA
[31] Space Research Institute, 84/32, Profsoyuznaya, Moscow 117997, Russia
[32] Department of Planetary Sciences, University of Arizona, Tucson, AZ 85721, USA
[33] MPE, Giessenbachstrasse, Postfach 1312, D-85748 Garching, Germany
[34] Observatoire de Paris, 10 rue Alice Domon et Leonie Duquet, F-75205 Paris Cedex 13, France
Received 2014 February 13; accepted 2015 April 5; published 2015 June 2

ABSTRACT

Gamma-ray bursts (GRBs) are characterized by ultra-relativistic outflows, while supernovae are generally characterized by non-relativistic ejecta. GRB afterglows decelerate rapidly, usually within days, because their low-mass ejecta rapidly sweep up a comparatively larger mass of circumstellar material. However, supernovae with heavy ejecta can be in nearly free expansion for centuries. Supernovae were thought to have non-relativistic outflows except for a few relativistic ones accompanied by GRBs. This clear division was blurred by SN 2009bb, the first supernova with a relativistic outflow without an observed GRB. However, the ejecta from SN 2009bb was baryon loaded and in nearly free expansion for a year, unlike GRBs. We report the first supernova discovered without a GRB but with rapidly decelerating mildly relativistic ejecta, SN 2012ap. We discovered a bright and rapidly evolving radio counterpart driven by the circumstellar interaction of the relativistic ejecta. However, we did not find any coincident GRB with an isotropic fluence of more than one-sixth of the fluence from GRB 980425. This shows for the first time that central engines in SNe Ic, even without an observed GRB, can produce both relativistic and rapidly decelerating outflows like GRBs.

Key words: gamma-ray burst: general – radiation mechanisms: non-thermal – shock waves – supernovae: individual (SN 2012ap) – techniques: interferometric

1. INTRODUCTION

1.1. Ordinary Supernovae

The optical light curves of supernovae have been well described by Arnett (1982) as a nearly blackbody photosphere which recedes into the ejecta, heated by γ-rays from nuclear decay and cooled by rapid expansion with a characteristic velocity of $v \sim 10^4\,\mathrm{km\,s^{-1}}$. The interaction of the ejecta with the circumstellar medium set up by the stellar wind of the progenitor star has been described by Chevalier (1982) using self-similar solutions. Such solutions have also successfully described the radio emission from SNe Ic (Chevalier 1998). The combination of nearly free expansion leading to decreasing optical thickness from free–free or synchrotron self absorption (SSA) and decreasing magnetic fields produces a decreasing peak frequency (the frequency at which the peak in the radio spectrum occurs), but a nearly constant flux density at the peak frequency (Chevalier 1998). In the self-similar solution, this interaction produces a shock front which expands in a power-law fashion with $R \propto t^m$, where R is the radius of the shockfront, t is the time since shock breakout, and m is known as the expansion parameter (also sometimes called the deceleration parameter). In the case of SNe Ib/c, which generally have a relatively tenuous circumstellar medium, this interaction produces little deceleration, and m is close to 1. The ejecta would slow down significantly only after encountering a mass of external medium comparable to the $\sim 1\,M_\odot$ of ejecta expected for SNe Ib/c supernovae. This Sedov time (Taylor 1950) is expected to be $\gtrsim 10^2$ years for supernovae. Therefore, young supernovae are usually found in a Newtonian phase of nearly free expansion.

1.2. Gamma-ray Bursts

Gamma-ray bursts (GRBs) were discovered by Klebesadel et al. (1973) using the *Vela* satellites, designed for the detection of nuclear tests in space. Ultra-relativistic blast waves had already been described by fluid dynamical Blandford & McKee (1976) solutions before they were implicated in the production of GRBs (Goodman 1986; Paczynski 1986). The production of GRBs requires that the ejecta have initial bulk Lorentz factors of $\Gamma \gtrsim 10^2$ (Piran 1999) in order to overcome the pair production opacity (Ruderman 1975; Schmidt 1978). Furthermore, even a small number of baryons in the initial ejecta can soak up most of the explosion energy available for γ-rays (Shemi & Piran 1990). This is referred to as baryon poisoning. Therefore, GRB jets must have $\lesssim 10^{-6}\,M_\odot$ of relativistic ejecta (Piran 1999) after breakout from the stellar progenitor surface, so as not to be baryon poisoned. In a short time, this relatively small mass of ejecta encounters a larger mass of external matter. Therefore, GRB afterglows are found in a relativistic but rapidly decelerating phase and have $\Gamma \lesssim 20$. The broad-lined (high velocity) type Ic SN 1998bw was discovered in the direction of GRB 980425 (Galama et al. 1998), and was characterized by the bright radio emission from its relativistic ejecta which had $\Gamma \sim 2$–3 (Kulkarni et al. 1998). This association between an SN Ic and a long GRB was followed by other supernovae like that of GRB 030329 with SN 2003dh (Hjorth et al. 2003) and XRF 060218 with SN 2006aj (Pian et al. 2006; Soderberg et al. 2006) also associated with GRBs. Some of these supernovae were marked by broad lines or by asphericity. However, the definitive property of this small subset of SNe Ic which allowed them to produce relativistic outflows remains elusive.

1.3. Search for Relativistic Ejecta

This evidence of a supernova–GRB connection inspired a systematic search for relativistic ejecta from nearby SNe Ic using radio observations, leading to the discovery of SN 2009bb by Soderberg et al. (2010) with $\gtrsim 10^{49}$ erg of energy in radio emitting relativistic ejecta. Like GRBs, SN 2009bb had relativistic ejecta (Soderberg et al. 2010), but this ejecta continued to be in nearly free expansion for $\sim$1 year (Bietenholz et al. 2010; Chakraborti et al. 2011), leading to the suggestion that, unlike GRBs, it is baryon loaded (Chakraborti & Ray 2011). Chakraborti et al. (2011) suggested that such engine-driven relativistic supernovae can even accelerate ultra-high-energy cosmic rays. Such a baryon loaded fireball was also implied in PTF11agg (Cenko et al. 2013). A rapid decline in flux density, faster than $\propto t^{-1}$ at a given radio frequency, or a decreasing peak flux density may signal the deceleration of the ejecta. Recently, the rapidly declining PTF12gzk was observed with $\lesssim 10^{46}$ erg of energy in its fast ejecta (Horesh et al. 2013). So far, however, highly energetic ($\gtrsim 10^{49}$ erg) relativistic ejecta combined with rapid deceleration has never been observed in a supernova unassociated with a GRB.

2. DISCOVERY OF SN 2012AP

SN 2012ap was discovered in NGC 1729 by the Lick Observatory Supernova Search (Jewett et al. 2012) on 2012 February 10. NGC 1729 is located at a distance of $D \sim 40$ Mpc (Springob et al. 2007) and we will assume a distance of 40.0 Mpc in what follows, although we note the dependence on distance where appropriate. The host galaxy was observed on 2012 February 5 and the supernova was not yet detected on that date. Therefore, the explosion must have occurred either after or at most a few days before this date. Spectroscopically, it was identied as an SN Ic with broad lines and marked by similarities with SN 2009bb and the GRB-associated SN 1998bw (Milisavljevic et al. 2012). Milisavljevic et al. (2014a) reported unusually strong diffuse interstellar bands in its optical spectra. Margutti et al. (2014) report on the non-detection of X-ray emission, and therefore indicate a short-lived central engine. Milisavljevic et al. (2014b) models the optical emission from the supernova and infer an explosion date of February 5 with an uncertainty of 2 days.

We detected strong radio emission from the supernova using the Karl G. Jansky Very Large Array (VLA) on 2012 February 15.0 UT with a steep inverted spectrum between 5.0 and 6.75 GHz. The subsequent radio observations using the VLA and the Giant Metrewave Radio Telescope (GMRT) showed an SSA spectrum (see Figure 1). See Section 3.1 for details on the radio observations and modeling. The peak flux densities and peak frequencies are summarized in Table 1.

3. OBSERVATIONS

In this section, we describe the observations of SN 2012ap obtained at various wavelengths. The first broadband radio spectrum was obtained at an age of 12 days. The radio data was well described with an SSA spectrum (see Figure 1). This allowed us to estimate the radius of the emission region (Chevalier 1998) to be $\sim 10^{16}$ cm. The inferred size evolution

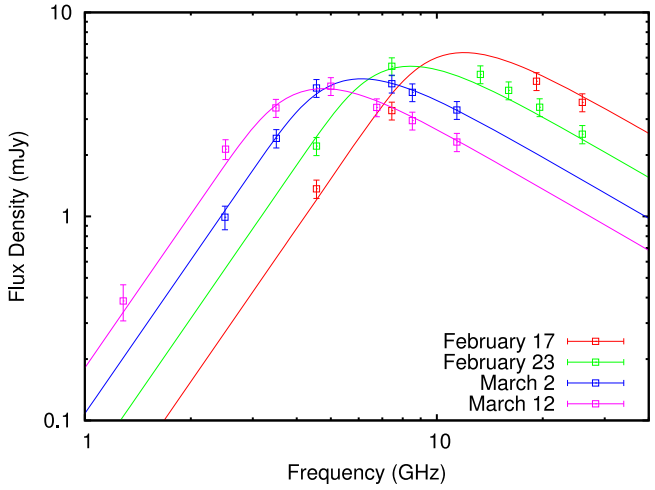

Figure 1. Temporal and spectral flux density evolution: radio observations of SN 2012ap were obtained using the VLA and GMRT. A simple synchrotron spectrum, with a low-frequency turnover due to SSA (Chevalier 1998) can explain the emission at all epochs discussed here. Note that the peak frequency decreases with time, similar to that of ordinary radio supernovae. In contrast to what is observed in ordinary supernovae, however, the peak flux density also decreases with time.

as a funtion of time is shown in Figure 2. The expanding ejecta may have slowed down since the time of explosion, and therefore this size gives us a lower limit on the initial apparent expansion velocity of $0.4\,c$. This is much faster than all other >100 nearby SNe Ibc in our sample (Soderberg et al. 2010), apart from SN 2009bb. Hence, SN 2012ap was chosen for detailed follow-up as the second relativistic supernova ever found without an associated GRB. This prompted a search for a high-energy counterpart using data from all of the spacecrafts within the InterPlanetary Network (IPN), a group of spacecrafts equipped with gamma-ray detectors for localizing GRBs (Hurley et al. 2009). The locations of the transients are determined by comparing the arrival times of the γ-rays at the different spacecraft. In the plausible range of explosion dates, 2012 February 5–10, there is no evidence of a GRB associated with SN 2012ap down to the IPN threshold of 6×10^{-7} erg cm^{-2}. We looked for transients with even lower fluences using *Fermi* and *Swift*, but we found none having small error boxes consistent with the position of the supernova.

3.1. Radio Temporal Evolution

No supernova was seen in the host galaxy on a pre-explosion image taken by the Katzman Automatic Imaging Telescope on February 5 down to an upper limit of 18.7 R magnitude. A subsequent image taken on February 10, revealed SN 2012ap at 17.3 R magnitude. We therefore conclude that the explosion happened before February 10, but not much before February 5. Since one of the major claims of this work is a deceleration, we count the age of the supernova from the February 5, which is near the beginning of this range. Later dates would imply even more deceleration. Milisavljevic et al. (2014b) models the optical light curve and provides an explosion date of February 5 ± 2, which is used in this work and interpreted as a 1σ bound on the explosion date. The present uncertainties of a few days in the explosion date dominates the uncertainty in m.

Both the VLA and GMRT observations have been reduced using Astronomical Image Processing Software (AIPS) standard techniques. Radio frequency interference in data was flagged and the interferometric visibilities were amplitude and phase calibrated. Bandpass calibration was performed using BPASS based on the flux calibrators 3C48 and/or 3C147. The single source data was extracted using the AIPS task SPLIT after final bandpass and flux calibration. The single source data sets were imaged using IMAGR. The images were corrected for the residual phase calibration errors using self-calibration of visibility phases (Cornwell & Fomalont 1989). The source flux densities were extracted by fitting Gaussian using the task JMFIT assuming point sources. The errors reported on the flux density are obtained by using the image statistics from the region surrounding the source.

These radio observations were used to obtain the values reported in Table 1 and in Figures 2 and 3. Quoted uncertainties in flux densities are statistical. There may be up to 5% systematic uncertainty from flux density calibration. This dominates the error budget quoted in the final derived values for E_0 and $\dot{M}$.

The full set of radio observations were fit with an SSA model with $p = 3$, as has been observed in SNe Ic. Both the peak flux density and peak frequency were allowed to vary as arbitrary power laws with an origin at February 6. A good global fit is obtained with a $\chi^2 = 0.98$ per degree of freedom. See Figure 1 for all of the radio observations and the fit. The radii (Figure 2) and magnetic fields (Figure 3) reported in Table 1 are derived from fits to the data at individual epochs.

The dependence of R on the ratio ϵ_e/ϵ_B and f are through a power of 1/19, and so they are likely to introduce only a negligible systematic uncertainty (Chevalier 1998). The dependence on distance is with a power 18/19, which could introduce a systematic shift but would not change the expansion parameter. The dependence on the flux density is a power of 9/19, and so a 5% error in flux density will add 2.5% of systematic error to the radii. These errors should be considered above and beyond the statistical uncertainties reported in the table. However, none of these are large enough to significantly change the results reported in this work.

3.2. Search for a High-energy Counterpart

Between 2012 February 05 and 2012 February 10, including both days, a total of five bursts were detected by one or more of the nine spacecraft of the (IPN: *Mars Odyssey, Konus-Wind*, *RHESSI*, *INTEGRAL* (SPI-ACS), *Swift* BAT, *Suzaku*, *AGILE, MESSENGER, and Fermi* (GBM)). All of these confirmed bursts were observed by more than one instrument on one or more spacecraft, and could be localized at least coarsely. During the same period, there were also three unconfirmed bursts which were observed by one experiment on one spacecraft (the 20 detector Suzaku HXD-WAM) in the triggered (TRN) mode. Their origin is uncertain; they could be cosmic or solar, but were too weak to be detected by other IPN spacecraft. In at least one case, it could be particle-induced. They cannot be localized accurately, but analysis of the detector responses indicates that they are unlikely to have originated from the direction of SN 2012ap. Therefore, they were excluded from further analysis. No bursts from known sources such as AXPs and SGRs were recorded during this period.

The completeness of our sample can be estimated as follows. We have three distinct sets of events: IPN bursts, Fermi GBM-only bursts, and bursts observed by the *Swift* BAT only within its coded field of view. The IPN is sensitive to bursts with

Table 1
Radius-magnetic Field Evolution

Observation Date (2012)	Age (Days)	$F_{\nu\ p}$[a] (mJy)	ν_p (GHz)	R (10^{15}cm)	B (mG)
February 17.0	12.0	5.85 ± 0.58	11.82 ± 0.48	10.7 ± 0.7	1084 ± 46
February 23.2	18.2	5.69 ± 0.07	8.92 ± 0.08	14.0 ± 0.2	820 ± 8
March 02.0	27.0	4.71 ± 0.10	6.13 ± 0.09	18.7 ± 0.3	576 ± 8
March 12.9	37.9	4.20 ± 0.10	4.54 ± 0.10	23.9 ± 0.6	431 ± 9

[a] Peak flux densities and peak frequencies of SN 2012ap are determined from our VLA and GMRT observations by fitting an SSA spectrum to the observed flux densities. Radius and magnetic fields are determined assuming equipartition (a possible source of systematic error). Quoted errors are statistical 1σ uncertainties.

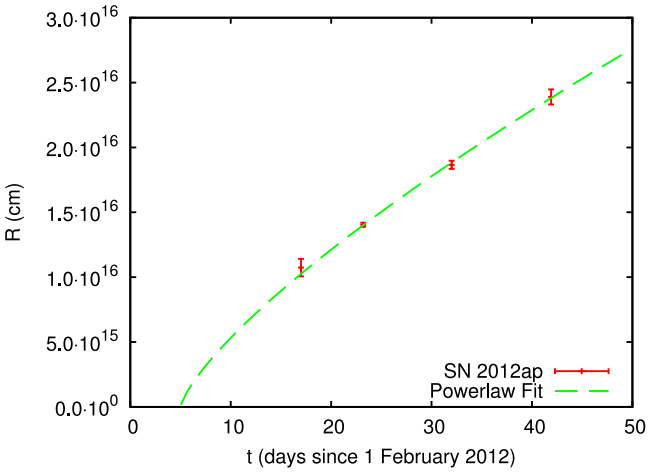

Figure 2. Temporal size evolution: radii were determined by fitting an SSA spectrum (Chevalier 1998) to the flux densities at each individual epoch. We assumed an explosion date of 2012 February 5 for this fit.

fluences down to about 6×10^{-7} erg cm^{-2}, and observes the entire sky with a temporal duty cycle close to 100% (Hurley et al. 2009). This places a threshold of $\sim 10^{47}$ erg on the isotropic equivalent γ-ray energy of any possibly GRB accompanying SN 2012ap if it were to be detected by the IPN. This is a factor ~6 lower than that of GRB 980425 accompanying SN 1998bw.

The *Fermi* GBM detects bursts down to an 8–1000 keV fluence of about 4×10^{-8} erg cm^{-2}, and observes the entire unocculted sky (8.8 sr) with a temporal duty cycle of more than about 86%. The weakest burst observed by the BAT within its coded field of view had a 15–150 keV fluence of 6×10^{-9} erg cm^{-2}, and the BAT observes a field of view of about 2 sr with a temporal duty cycle of about 90%. Generally, the weakest bursts are short-duration GRBs; higher fluences characterize the sensitivities to long-duration GRBs.

The localization accuracies of the five confirmed bursts varied widely. None were observed within the coded fields of view of the *Swift* BAT, *INTEGRAL* IBIS, or Super-AGILE (several arcminute accuracy). None were observed by MAXI (several degree accuracy). Two were observed either by the *Fermi* GBM alone, or by the *Fermi* GBM and one near-Earth spacecraft (so that they could not be localized accurately by triangulation). These bursts had 1σ statistical-only error radii of 23.8° and 5.5°. The GBM error contours are not circles, although they are characterized as such, and have about 3.2° of systematic uncertainties associated with them. Adding the statistical and systematic uncertainties in quadrature provides a reasonable approximation to a 1σ error circle, and multiplying that radius by 3 gives a reasonable approximation to a 3σ (statistical and systematic) error circle. These two *Fermi* bursts have positions that are inconsistent with that of the SN (that is, the SN falls far outside the 3σ error circle as approximated above). Two were observed by interplanetary and near-Earth spacecraft, and could be triangulated to small error boxes whose positions exclude the position of SN 2012ap. One burst was observed by the *Swift* BAT outside the coded field of view, and by the *INTEGRAL* SPI-ACS. As the distance between these two spacecraft is only about 0.5 lt-s, the event can be triangulated, but not accurately. Its error annulus has an area of 1.8 sr, which includes the position of the supernova. The total area of the localizations of the five confirmed bursts was 0.5 times 4 pi sr. This implies that about 0.5 bursts can be expected to have positions which are consistent with any given point on the sky simply by chance (i.e., within the 3σ error region). In our sample, one burst has a position consistent with the SN position (Poisson probability 0.3).

There is another approach to the probability calculation. Since only 0 or 1 GRB in our sample can be physically associated with the supernova, we can calculate two other probabilities. The first is the probability that in our ensemble of five bursts, none is associated by chance with the supernova. For our ensemble, this probability is 0.54. The second probability is that any one burst is associated by chance with the SN, and that all the others are not. For our ensemble, that probability is 0.39. Since we find approximately the expected number of chance coincidences, and since there are no bursts with small error boxes whose positions are consistent with the supernova, there is no strong evidence for an SN-associated GRB within the time window down to the IPN threshold. If the supernova produced a burst below the IPN threshold and above the *Fermi* one, then it is possible that both *Swift* and *Fermi* would not detect it; considering their spatial and temporal coverages, the joint non-detection probability is about 0.38. Finally, if the supernova produced a burst below the *Fermi* threshold but above the *Swift* one, then the probability is about 0.86 that it would not be detected.

In summary, no confirmed coincident burst with an isotropic fluence of more than one-sixth of GRB 980425 was localized to the direction of SN 2012ap within the relevant time window. Weaker bursts were searched for, albeit with <100% duty cycle, but also not found.

4. INTERPRETATION

In this section, we describe what conclusions can be made concerning the explosion, its energy budget, and its environments based on the observations described above.

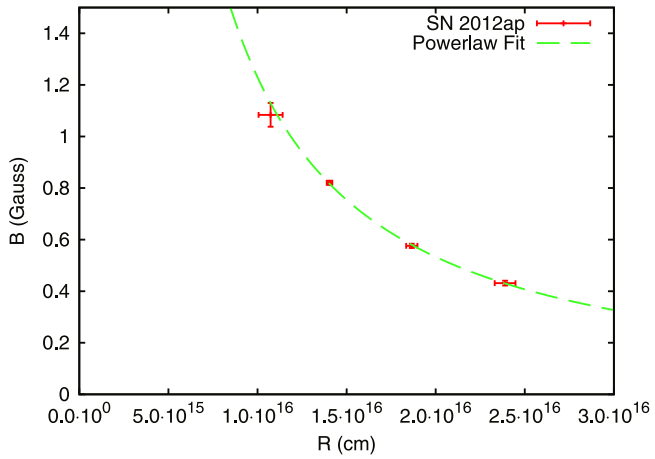

Figure 3. Magnetic field evolution: radii and magnetic fields were determined by fitting an SSA spectrum (Chevalier 1998) to the flux densities at each individual epoch.

4.1. Deceleration

As a supernova expands, its radio emitting region becomes optically thinner. The expansion also dilutes the energy density of relativistic electrons and magnetic fields. In the nearly free expansion phase, these two effects conspire (Chevalier 1998; Chakraborti & Ray 2011) to decrease the turnover frequency of the SSA spectrum but keep the peak flux density nearly constant in time. In the case of SN 2012ap, the peak flux density fell steadily over the first month of observations (see Figure 1) and the expansion is well fit by a power law of the form, $R \propto t^{m}$, where $m = 0.74 \pm 0.03$. Here, the 1σ statistical uncertainty is derived from the radio size determinations following Chevalier (1998). However, the determination of the explosion date derived from optical observations (Milisavljevic et al. 2014b) presents a greater 1σ systematic uncertainty of 0.07. This is determined by refitting the data with the range of explosion dates allowed by the optical studies of the supernova. Taking both into account and summing them in quadrature, the total uncertainly in m is 0.08. Therefore, our estimate of the expansion parameter is $m = 0.74 \pm 0.08$, which incorporates our understanding of the statistical and systematic uncertainties dominated by the radio observations and time of explosion, respectively. This is 3σ away from the value near 1 expected for undecelerated expansion.

The combination of the high velocity and small expansion parameter place SN 2012ap at an unique position in Figure 4 Within the context of an ordinary SN Ic, this would imply a supernova ejecta density profile characterized by a power-law distribution of mass ejected at a particular velocity $\propto v^{-6}$, where v is the velocity. However, the expulsion of stellar envelopes is expected to produce much steeper ejecta profiles (Matzner & McKee 1999). This could plausibly be explained by an extraordinarily energetic supernova with a low ejecta mass and a shallow ejecta profile extending into relativistic velocities. Our observations of SN 2012ap imply much more energy coupled to high-velocity ejecta than is expected from realistic explosion models of ordinary core collapse supernovae. The decelerating expansion is, however, consistent with a Central Engine Driven EXplosion (CEDEX; Chakraborti & Ray 2011), which places a large amount of energy in a small mass of relativistic ejecta responsible for the radio afterglow which separates itself from the non-relativistic ejecta responsible for the optical emission. The decelerating expansion of this component interacting with the wind of the progenitor star is expected to produce (see appendix) a $R \propto t^{3/4}$ behavior consistent with the observations.

4.2. Total Energy Budget

Within the context of such a CEDEX, our radio observations allow us to perform calorimetry on the fireball responsible for this radio afterglow. The initial energy in the relativistic component can be estimated as (see the appendix for derivation and assumptions)

$$E_0 = 1.45 \times 10^{45} \left(\frac{F_{\nu p}}{\mathrm{mJy}}\right)^{23/19} \left(\frac{\nu_p}{\mathrm{GHz}}\right)^{-1} \left(\frac{D}{\mathrm{Mpc}}\right)^{46/19} \mathrm{erg}. \quad (1)$$

Using the SSA spectral fits from age 18 days, the epoch with the smallest fractional uncertainties in peak flux density $F_{\nu p}$ and peak frequency ν_p, we estimate $(1.0 \pm 0.1) \times 10^{49}$ erg of energy in the relativistic ejecta. This estimate is robust, irrespective of whether one chooses a relativistic or Newtonian blastwave model. This energy is comparable to the energy observed in the relativistic outflows from SN 2009bb and supernovae such as SN 1998bw associated with sub-energetic GRBs in the local universe. This energy estimate forces the plausible combinations of ejected mass and initial velocity (see Figure 5) to lie in a narrow region above and parallel to the magenta line for 10^{49} erg.

4.3. Circumstellar Density

In addition, the model allows us to derive (see the appendix) the mass loss rate of the progenitor responsible for the circumstellar interaction. Again, using the data from age 18 days, we estimate the pre-explosion mass loss rate between 6.0×10^{-6} and $6.5 \times 10^{-5}\, M_{\odot}\ \mathrm{yr}^{-1}$, depending on whether one uses a relativistic or Newtonian blastwave model, respectively. This range of values is consistent with the expected mass loss rate of Wolf–Rayet stars (Nugis & Lamers 2000) and is comparable to the case of SN 2009bb (Soderberg et al. 2010). The upper limit on the mass loss rate, derived by Margutti et al. (2014) using X-ray non-detection from the *Chandra* X-ray observations, rules out the higher mass loss rate derived from the non-relativistic model. This encourages us to prefer the lower of these values. Hence, we prefer the relativistic blaswave model. Since we find the radio afterglow of SN 2012ap in a decelerating phase, its relativistic outflow must have already swept up a mass of circumstellar matter greater than its own mass. This can place an upper limit on the mass of the relativistic ejecta, which is easily estimated since we have already determined the circumstellar density and blastwave radius. This argument constrains the mass of the relativistic ejecta to be $\lesssim 1.2 \times 10^{-5}\, M_{\odot}$. This restricts the allowed range of initial parameters for SN 2012ap (see yellow box in Figure 5). Hence, the mass of the ejecta component powering the radio afterglow of SN 2012ap is much less than that responsible for the optical light curve of a typical supernova and closer to the estimated mass of the relativistic component of a GRB's ejecta.

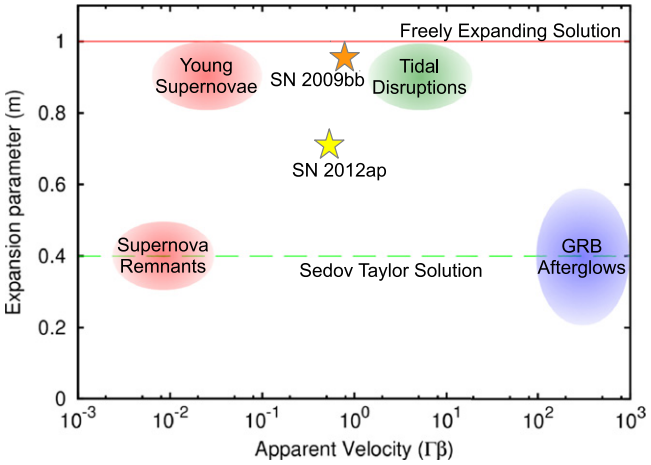

Figure 4. Phase space of afterglows: explosions are classified in this cartoon diagram by the apparent expansion velocity $\Gamma\beta$ in natural units and the dimensionless expansion parameter m (where $R \propto t^m$) of the component driving the radio afterglow. Explosion parameters on the red line correspond to freely expanding solutions in which the expansion velocity is constant in time. Explosions on the green line are in a Sedov Taylor phase (Taylor 1950). GRB afterglows are found in the lower right portion corresponding to a ultra-relativistic decelerating Blandford & McKee (1976) phase. We indicate the location of supernovae and novae with standard parameters. SN 2009bb was discovered to be mildly relativistic and in nearly free expansion. SN 2012ap parameters are determined from radio observations in this work. The sizes of the blobs represent the typical variation within that class and the sizes of the stars represent their individual uncertainties. Note that SN 2012ap populates a hitherto unpopulated phase space.

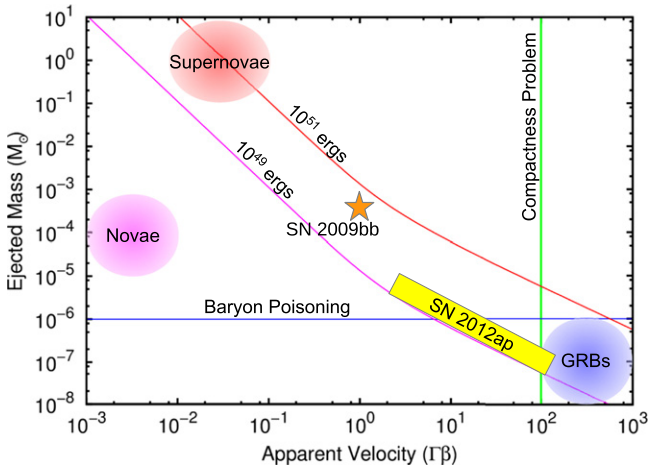

Figure 5. Phase space of explosions: explosions are classified in this cartoon diagram by their apparent expansion velocity and ejecta mass responsible for their electromagnetic display. Everything to the left of the green dashed line suffers from the "compactness problem" (Ruderman 1975; Schmidt 1978) and no γ-rays can get out due to pair production opacity. Everything above the blue line is "baryon poisoned" (Shemi & Piran 1990) and cannot produce γ-rays as the baryons take up much of the energy. Therefore, GRBs are confined to the lower right corner. We indicate the location of supernovae and novae with standard parameters. SN 2009bb was discovered to be mildly relativistic and baryon loaded. SN 2012ap parameters are from blastwave calorimetry in this work. The red line indicates an explosion energy of 10^{51} erg and the magenta line indicates 10^{49} erg. Note that SN 2012ap occupies a hitherto unpopulated region of phase space in the continuum between supernovae and GRBs, between SN 2009bb and GRBs.

5. DISCUSSION

Even though no GRB counterpart was found for SN 2012ap, its radio afterglow shares remarkable characteristics with those of GRB-associated supernovae; it has a relativistic ejecta component with relatively few baryons. While SN 2009bb had a relativistic outflow, it was clearly baryon loaded which is not the case here. A rapid radio decline was observed in PTF12gzk which may also have had fast ejecta. However, SN 2012ap had orders of magnitude more energy in relativistic ejecta, placing its energetics firmly in the class of GRB-associated supernovae. SN 2012ap pushes the boundaries of explosion parameters observed from stripped core progenitors with central engines (see Figures 4 and 5). The parameters that separate the outflows, from GRB-associated supernovae and ordinary SNe Ib/c, according to Chakraborti & Ray (2011) are the velocity and baryon loading of their fastest ejecta. According to Margutti et al. (2014), the duration of the central engine activity drives the diversity of the explosion outcomes. By bridging the gap between ordinary supernovae and GRB-associated supernovae in terms of its high velocity and low ejecta mass, SN 2012ap demonstrates the role of CEDEXs in understanding the supernova–GRB connection.

This work made use of radio observations from the NRAO VLA and GMRT. The National Radio Astronomy Observatory is a facility of the National Science Foundation operated under cooperative agreement by Associated Universities, Inc. We thank the staff of the GMRT that made these observations possible. GMRT is run by the National Centre for Radio Astrophysics of the Tata Institute of Fundamental Research. The Konus-WIND experiment is partially supported by a Russian Space Agency contract, RFBR grants 15-02-00532a and 13-02-12017 ofi-m. We thank Roger Chevalier and Ehud Nakar for comments.

APPENDIX A
BLASTWAVE EVOLUTION

We follow the derivation of the blastwave evolution derived for CEDEX (Chakraborti & Ray 2011). We consider a simple collisional model (Chiang & Dermer 1999; Piran 1999) where the relativistic ejecta interacts with the circumstellar matter and forms a decelerating shell. The ejecta is characterized by the rest frame mass M_0 of the shell launched by CEDEX and its initial Lorentz factor γ_0. The total energy is given by $E_0 = \gamma_0 M_0 c^2$. For a progenitor with a mass loss rate of $\dot{M}$ through a wind with velocity v_w, the ejecta sweeps up AR (where $A \equiv \dot{M}/v_w$ and the circumstellar density falls off as $\propto R^{-2}$) amount of circumstellar matter within a radius R. This slows down the ejecta, whose Lorentz factor evolves as

$$\gamma = \left(\frac{\gamma_0 M_0}{} + \frac{-M_0 + 2Ac\gamma_0 t + \sqrt{8\,AcM_0 t\gamma_0^3 + \left(M_0 - 2Ac\gamma_0 t\right)^2}}{2\gamma_0} \right) \Bigg/ \sqrt{\left(2\,Ac\gamma_0 t + \sqrt{8\,AcM_0 t\gamma_0^3 + \left(M_0 - 2Ac\gamma_0 t\right)^2}\right) M_0 + \frac{\left(-M_0 + 2Ac\gamma_0 t + \sqrt{8\,AcM_0 t\gamma_0^3 + \left(M_0 - 2Ac\gamma_0 t\right)^2}\right)^2}{4\gamma_0^2}}, \quad (2)$$

according to Chakraborti & Ray (2011).

For both the prototypical SN 2009bb and the newly discovered SN 2012ap, the blastwave was not ultra-relativistic at the time of the observed radio afterglow. Without a large relativistic beaming effect, the observer would receive emission from the entire shell of apparent lateral extent $R_{\rm lat}$ at a time $t_{\rm obs}$ given by

$$dt_{\rm obs} = \frac{dR_{\rm lat}}{\beta\gamma c}. \quad (3)$$

Radio observations of SN 2012ap essentially measure this transverse $R_{\rm lat}$, not the line of sight R. Substituting $\beta\gamma$ using Equation (2) and integrating gives us a large and unintuitive expression for $R_{\rm lat}(t)$ which is not quoted here. Since we find SN 2012ap in a decelerating phase, we take the limit of $M_0 \to 0$, holding E_0 constant. This brings us to the portion of the full solution where the swept up mass is more than the ejecta mass. Furthermore, since the explosion is still relativistic, we know that we are still in the early phase, and therefore expand the solution as a power series around $t = 0$. This gives us the intermediate asymptotic solution for the lateral expansion of the blastwave in its decelerating but relativistic phase as

$$R_{\rm lat} = \left(\frac{cE_0}{8A}\right)t^{3/4} + \mathcal{O}\left(t^{5/4}\right). \quad (4)$$

We suggest that this explains the $R \propto t^{3/4}$ evolution of the apparent size of SN 2012ap.

APPENDIX B
RADIO EMISSION

The radio emission is powered by synchrotron losses suffered by accelerated electrons in shock amplified magnetic fields. Assuming that a fraction ϵ_e of the total energy is used to accelerate electrons into a power law with index $p = 3$ extending from γ_m to ∞, filling a fraction f of the volume, gives us the normalization of the electron distribution as

$$N_0 = \frac{3\epsilon_e E_0\left(\gamma_m m_e c^2\right)}{4\pi\, fR^3}. \quad (5)$$

Similar assumptions give the average magnetic field as

$$B = \sqrt{\frac{6\epsilon_e E_0}{fR^3}}. \quad (6)$$

Once we have the evolution of N_0 and B, we can obtain the optically thick and thin portions of the SSA spectrum as (Rybicki & Lightman 1979)

$$F_\nu = \frac{\pi R^2}{D^2}\frac{c_5}{c_6}B^{-1/2}\left(\frac{\nu}{2c_1}\right)^{5/2}, \quad (7)$$

and

$$F_\nu = \frac{4\pi\, fR^3}{3D^2}c_5 N_0 B^{(p+1)/2}\left(\frac{\nu}{2c_1}\right)^{-(p-1)/2}, \quad (8)$$

respectively, where c_1, c_5, and c_6 are constants (Pacholczyk 1970) and D is the distance to the source. In mildly relativistic cases such as SN 2012ap, we may receive radiation from the entire disk projected on the sky, and hence R is to be understood as $R_{\rm lat}$. We then substitute for N_0 and B using Equations (5) and (6) and the leading-order expansion for the projected lateral radius using Equation (4). The optically thick and thin regimes meet at the turnover frequency of,

$$\nu_p = \frac{\left(4\ 2^{33/56}3^{5/14}\left(\frac{A}{c}\right)^{23/56}c_1 E_0^{13/56}(c_6\epsilon_e)^{2/7} \times \left(\frac{\epsilon_B}{f}\right)^{5/14}\left(\gamma_m m_e c^2\right)^{2/7}\right)}{\left(\pi^{2/7}t^{69/56}\right)}, \quad (9)$$

with a flux density of

$$F_{\nu p} = \frac{4\ 4^{37/56}3^{9/14}\pi^{2/7}c_5\epsilon_e^{5/7}}{c_6^{2/7}D^2}\left(\frac{A}{c}\right)^{19/56} \times \left(\frac{\epsilon_B}{f}\right)^{9/14}\left(\gamma_m m_e c^2\right)^{5/7}\left(\frac{E_0}{t}\right)^{57/56}. \quad (10)$$

Such an evolution of the SSA spectrum is qualitatively similar to that of SNe Ibc, in that the peak flux density decreases with time for both of them. However, the way that the peak flux density decreases in this case is distinctly different, while it is nearly constant for supernovae in the nearly free expansion phase.

APPENDIX C
DIAGNOSTIC EXPRESSIONS

In practice, the parameters of the explosion are not known a priori, but the peak flux density and frequency can be determined through observations. Therefore, the above expressions must be inverted to solve for the explosion energy and circumstellar density from the observed parameters. The expression for the explosion energy is most useful when put in terms of observable quantities. We substitute the values of the constant c's and assume that $\epsilon_e = \epsilon_B = 0.01$ and $\gamma_m = 2$, as is appropriate for a mildly relativistic shock. This gives us

$$E_0 = 2.45 \times 10^{45}\left(\frac{F_{\nu p}}{\rm mJy}\right)^{23/19}\left(\frac{\nu_p}{\rm GHz}\right)^{-1}\left(\frac{D}{\rm Mpc}\right)^{46/19}\ {\rm erg}. \quad (11)$$

The circumstellar density can be derived in a similar fashion. Within the context of this relativistic blastwave model, this gives us

$$\dot{M} = 8.47 \times 10^{-10}\left(\frac{F_{\nu p}}{\rm mJy}\right)^{-13/19}\left(\frac{\nu_p}{\rm GHz}\right)^{3}\left(\frac{D}{\rm Mpc}\right)^{-26/19} \times \left(\frac{t}{\rm day}\right)^{3}\left(\frac{v_w}{10^3\ {\rm km\ s^{-1}}}\right)M_\odot\ {\rm yr}^{-1}. \quad (12)$$

We make a further assumption that the wind speed was $v_w = 1000$ km s^{-1} as is appropriate for a Wolf Rayet progenitor. Using the data from age 18 days, we estimate the pre-explosion mass loss rate as $(6.0 \pm 0.4) \times 10^{-6}\ M_\odot$ yr^{-1}.

The above model is strictly true for highly relativistic blastwaves, while the observed explosion is only mildly relativistic. We therefore also consider the Newtonian limit to

see if it gives systematically different results. The entire calculation can be redone in the context of the Newtonian Sedov-Taylor-like blastwave. The final result for the explosion energy remains the same, indicating that the calorimetric estimate of the explosion energy is robust. The expression for the circumstellar density changes to

$$\dot{M} = 1.88 \times 10^{-8} \left(\frac{F_{\nu p}}{\mathrm{mJy}}\right)^{-4/19} \left(\frac{\nu_p}{\mathrm{GHz}}\right)^{2} \left(\frac{D}{\mathrm{Mpc}}\right)^{-8/19} \times \left(\frac{t}{\mathrm{day}}\right)^{2} \left(\frac{v_w}{10^3\ \mathrm{km\ s^{-1}}}\right) M_\odot\ \mathrm{yr}^{-1}. \quad (13)$$

This gives us an estimate of $(6.5 \pm 0.4) \times 10^{-5}\, M_\odot\ \mathrm{yr}^{-1}$. The real mass loss rate may be between these two systematically different estimates. Upper limits on the mass loss rate from Margutti et al. (2014) rule out this higher mass loss rate and are consistent with the results from the relativistic model.

REFERENCES

Arnett, W. D. 1982, ApJ, 253, 785
Bietenholz, M. F., Soderberg, A. M., Bartel, N., et al. 2010, ApJ, 725, 4
Blandford, R. D., & McKee, C. F. 1976, PhFl, 19, 1130
Cenko, S. B., Kulkarni, S. R., Horesh, A., et al. 2013, ApJ, 769, 130
Chakraborti, S., & Ray, A. 2011, ApJ, 729, 57
Chakraborti, S., Ray, A., Soderberg, A. M., Loeb, A., & Chandra, P. 2011, NatCo, 2, 175
Chevalier, R. A. 1982, ApJ, 258, 790
Chevalier, R. A. 1998, ApJ, 499, 810
Chiang, J., & Dermer, C. D. 1999, ApJ, 512, 699
Cornwell, T., & Fomalont, E. B. 1989, in ASP Conf. Ser. 6, Synthesis Imaging in Radio Astronomy, ed. R. A. Perley, F. R. Schwab, & A. H. Bridle (San Francisco, CA: ASP), 185
Galama, T. J., Vreeswijk, P. M., van Paradijs, J., et al. 1998, Natur, 395, 670
Goodman, J. 1986, ApJL, 308, L47
Hjorth, J., Sollerman, J., Møller, P., et al. 2003, Natur, 423, 847
Horesh, A., Kulkarni, S. R., Corsi, A., et al. 2013, ApJ, 778, 63
Hurley, K., Cline, T., Mitrofanov, I. G., et al. 2009, AIP Conf. Ser. 1133, GAMMA-RAY BURST: Sixth Huntsville Symposium, ed. C. Meegan, C. Kouveliotou, & N. Gehrels (NewYork: AIP), 55
Jewett, L., Cenko, S. B., Li, W., et al. 2012, CBET, 3037, 1
Klebesadel, R. W., Strong, I. B., & Olson, R. A. 1973, ApJL, 182, L85
Kulkarni, S. R., Frail, D. A., Wieringa, M. H., et al. 1998, Natur, 395, 663
Margutti, R., Milisavljevic, D., Soderberg, A. M., et al. 2014, ApJ, 797, 107
Matzner, C. D., & McKee, C. F. 1999, ApJ, 510, 379
Milisavljevic, D., Margutti, R., Crabtree, K. N., et al. 2014a, ApJL, 782, L5
Milisavljevic, D., Margutti, R., Parrent, J. T., et al. 2014b, ApJ, 799, 51
Milisavljevic, D., Fesen, R., Soderberg, A., et al. 2012, CBET, 3037, 2
Nugis, T., & Lamers, H. J. G. L. M. 2000, A&A, 360, 227
Pacholczyk, A. G. 1970, in Radio astrophysics. Nonthermal processes in galactic and extragalactic sources (San Francisco, CA: Freeman)
Paczynski, B. 1986, ApJL, 308, L43
Pian, E., Mazzali, P. A., Masetti, N., et al. 2006, Natur, 442, 1011
Piran, T. 1999, PhR, 314, 575
Ruderman, M. 1975, Annals of the New York Academy of Sciences, Vol. 262, Seveth Texas Symposium on Relativistic Astrophysics, ed. P. G. Bergman, E. J. Fenyves, & L. Motz (NewYork: Wiley), 164
Rybicki, G. B., & Lightman, A. P. 1979, Radiative Processes in Astrophysics (NewYork: Wiley)
Schmidt, W. K. H. 1978, Natur, 271, 525
Shemi, A., & Piran, T. 1990, ApJL, 365, L55
Soderberg, A. M., Kulkarni, S. R., Nakar, E., et al. 2006, Natur, 442, 1014
Soderberg, A. M., Chakraborti, S., Pignata, G., et al. 2010, Natur, 463, 513
Springob, C. M., Masters, K. L., Haynes, M. P., Giovanelli, R., & Marinoni, C. 2007, ApJS, 172, 599
Taylor, G. 1950, RSPSA, 201, 159